



Prograde metamorphism, strain evolution, and collapse of footwalls of thick thrust sheets: a case study from the Mesozoic Sevier hinterland U.S.A.

PHYLLIS A. CAMILLERI

Department of Geology and Geophysics, University of Wyoming, Laramie, Wyoming, U.S.A. and
Department of Geology and Geography, Austin Peay State University, Clarksville, TN 37044, U.S.A.,
E-mail: camillerip@apsu01.cpsu.edu

(Received 3 January 1997; accepted in revised form 16 March 1998)

Abstract—Analysis of prograde metamorphic fabrics in the exhumed footwall of the Mesozoic Windermere thrust, northeast Nevada, reveals fabrics and style of ductile flow developed during tectonic burial metamorphism of a sedimentary footwall of a thick thrust sheet. In response to structural burial, footwall strata underwent Barrovian metamorphism synchronous with development of bedding-parallel or near parallel *S* and *S-L* tectonites. Footwall rocks range from unmetamorphosed at high structural levels and progressively increase in metamorphic grade to upper amphibolite facies at deep levels. Attenuation of footwall stratigraphic units accompanied tectonite development whereby the amount of attenuation varies with metamorphic grade from ~0% in lower greenschist facies to ~30–50% in upper amphibolite facies rocks. Microstructures in metacarbonate, metapsammite, and metapelite, and analysis of crystallographic preferred orientations of quartz *c*-axes in quartzite, suggest a dominantly coaxial strain path with flattening strain predominating at lower metamorphic grade and plane strain more dominant at higher metamorphic grade. The microstructural data indicate that dominantly coaxial deformation during metamorphism accommodated extension of the footwall. Ductile extension most likely records footwall collapse induced by a loss of strength due to relative upward migration of isotherms during and or following burial. Extension may act as a mechanism that in part facilitates isostatic accommodation or sinking of the overlying load resulting in a reduction of topography. Attenuation of footwalls of thick thrust sheets and production of predominantly coaxial layer-parallel or near parallel fabrics may be an intrinsic process once sufficient structural overburden is developed and thermal relaxation and prograde metamorphism ensues. © 1998 Elsevier Science Ltd. All rights reserved

INTRODUCTION

In continental contractional orogens, footwalls of large thrust sheets undergo flexure in response to loading (e.g. Turcotte and Schubert, 1982) and ultimately heating due to reequilibration of thermal gradients (Oxburgh and Turcotte, 1974; England and Thompson, 1984; Thompson and England, 1984). In tectonically thickened crust, such heating—or thermal relaxation—results in Barrovian style metamorphism, ductile flow, and production of foliated regional metamorphic rocks that record clockwise pressure–temperature paths (Oxburgh and Turcotte, 1974; England and Thompson, 1984; Thompson and England, 1984). Much attention has focused on assessing the pressure–temperature–time paths of Barrovian metamorphic terranes because this type of information is useful for inferring the magnitude and duration of thrust loading. However, little work has been done to assess the origin, geometry, and type of strain or ductile flow that develops during prograde metamorphism of a plate that has undergone flexure and heating in response to loading. Consequently, the significance of flow during prograde metamorphism, and its contribution to the rheological and structural evolution of internal zones, is poorly understood.

This paper presents an empirical, field-based structural study of the geometry, partitioning, and style of strain that accompanied prograde, tectonic-burial metamorphism in the footwall of the Windermere thrust (Camilleri and Chamberlain, 1997) in northeastern Nevada (Fig. 1). The footwall is ideally suited for study because it is a rare exposure of a nearly complete transition of unmetamorphosed and unfoliated rocks to high grade foliated metamorphic rocks, and the prograde metamorphic fabric within the footwall lacks a substantial overprint of polyphase fabrics so typical of most contractional orogens. The intent of this paper is two-fold. The first is to present a case study providing a complete middle to upper crustal geometric picture of the partitioning and type of strain that may accompany Barrovian style metamorphism of thick sedimentary sequences in response to burial by thrust faulting. The second is to assess the significance of flow during metamorphism of footwalls of thick thrust sheets in terms of their rheological, structural, and petrological evolution.

The results of this study suggest, that with sufficient loading, footwalls of thick thrust sheets ultimately lose their flexural strength and collapse by dominantly plastic coaxial flow directly beneath the load and that plastic extension is triggered by, and is a direct result of, thermal relaxation during and or following loading.

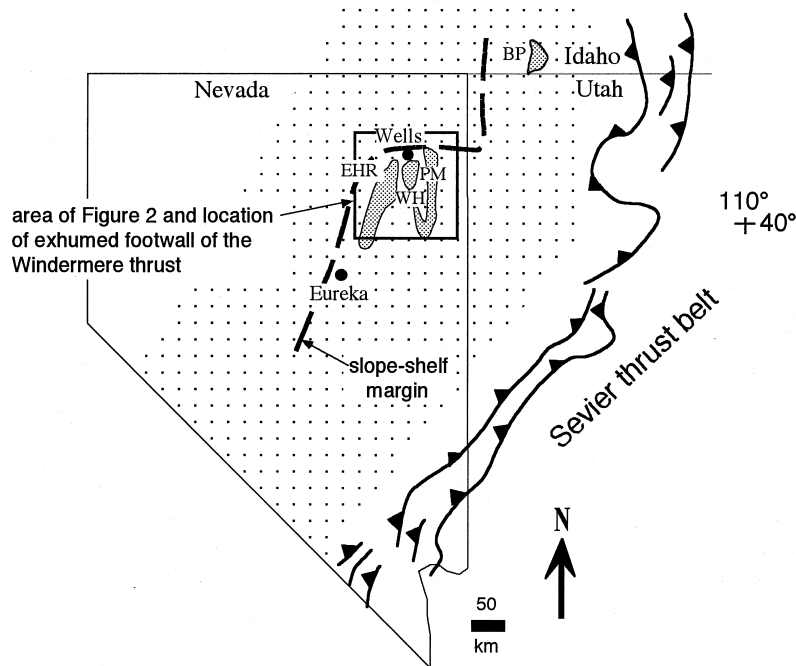


Fig. 1. Tectonic map of Nevada and western Utah showing the position of the Sevier fold and thrust front, its hinterland (stippled region), and the location of the area of study. EHR = East Humboldt Range; BP = Black Pine Mountains; WH = Wood Hills; PM = Pequop Mountains. Position of the slope-shelf margin is after Miller *et al.* (1991).

This process manifests itself as Barrovian-style metamorphism synchronous with development of a foliation that is parallel or at a low angle to bedding and which records dominantly coaxial deformation.

GEOLOGIC FRAMEWORK

The Windermere thrust is an inferred thrust that formed in the internal zone of the Sevier orogen (Fig. 1). The Sevier orogen is a Mesozoic to early Tertiary back-arc fold and thrust belt along the western margin of the North American continent. The Windermere thrust is a top-to-the-southeast thrust that duplicated a thick continental margin sequence composed of Precambrian to Mesozoic carbonate and siliciclastic strata. The footwall of the thrust was exhumed by top-to-the-west to west-northwest normal faults and is presently exposed in the Pequop Mountains, Wood Hills, and East Humboldt Range–Ruby Mountains region in northeast Nevada (Camilleri and Chamberlain, 1997; Figs 1 & 2). The Windermere thrust and its hanging wall were excised by the normal faults, and sparse, exposed remnants of the hanging wall of the thrust are present in the upper plates of low-angle normal faults. The exhumed footwall of the Windermere thrust ranges from unmetamorphosed to the east and south and progressively increases in metamorphic grade to the northwest (Fig. 2). Barometric data indicate that metamorphic

pressure increases to the northwest and that the metamorphic pressures recorded in various stratigraphic units greatly exceed premetamorphic pressures corresponding to inferred original stratigraphic depths (Camilleri and Chamberlain, 1997).

The region containing the exhumed footwall of the Windermere thrust represents a localized area of continental margin strata that underwent regional Barrovian metamorphism and is inferred to represent an area of localized, large magnitude crustal thickening that parallels a fundamental west-trending bend in the otherwise north-trending Late Proterozoic to Paleozoic slope-shelf margin (Miller and Hoisch, 1992; Camilleri *et al.*, 1992; Fig. 1). Miller *et al.* (1991) and Miller and Hoisch (1992) infer that the salient in the slope-shelf margin is a primary depositional feature that was controlled by an underlying west-trending tectonic boundary within Precambrian basement. They also infer that these crustal features subsequently caused localization of extreme shortening and thickening during the Mesozoic.

Prior to exhumation, the footwall of the Windermere thrust dipped to the northwest beneath a southeast tapering thrust wedge (Fig. 3a). A westerly dip of the footwall is inferred from barometric data from metamorphosed footwall units as well as by structural relationships (Camilleri and Chamberlain, 1997). Rocks within the footwall contain a Barrovian-style metamorphic sequence; strata are unmetamorphosed at high structural levels and progressively

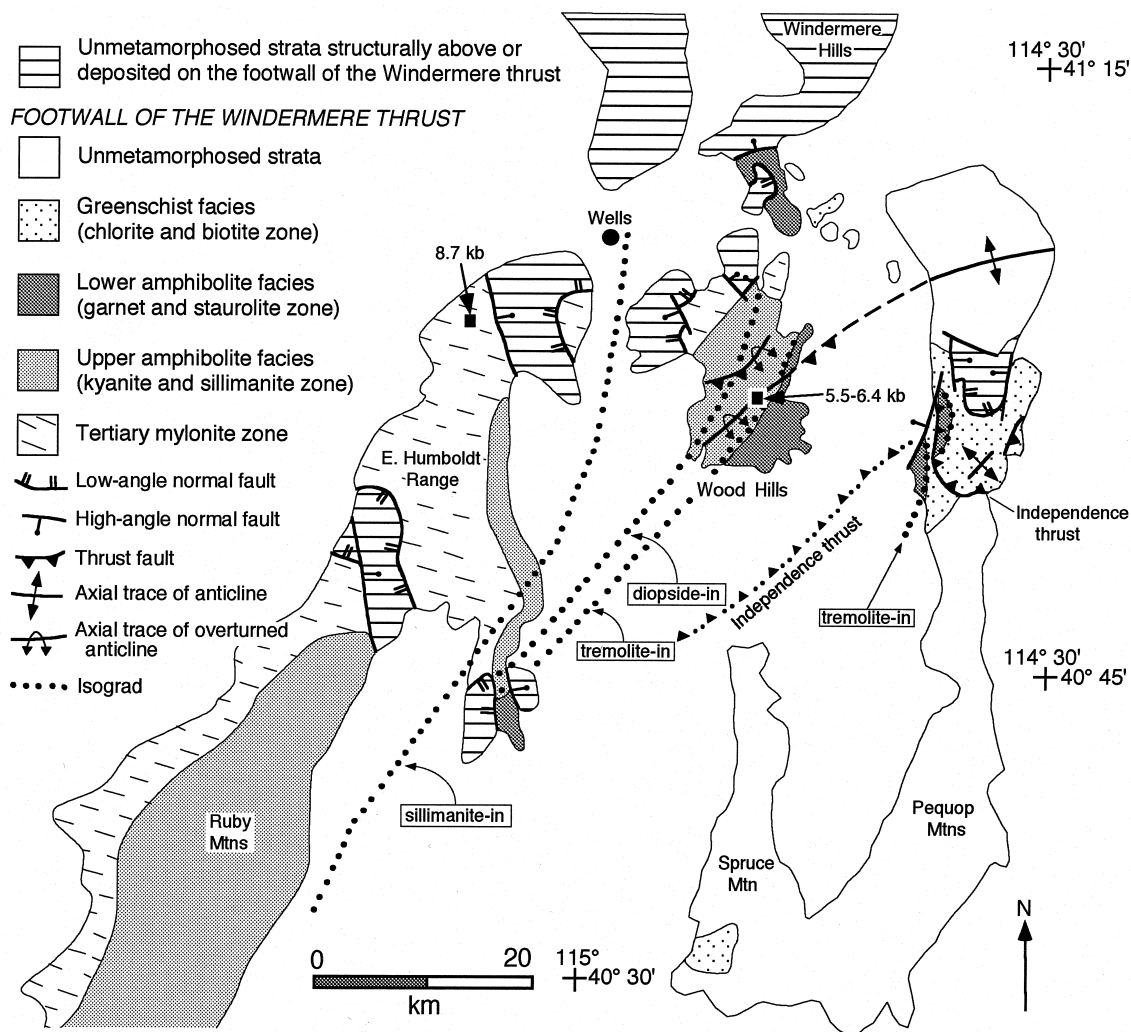


Fig. 2. Simplified tectonic and metamorphic map of the Pequop Mountains, Wood Hills, Spruce Mountain, Ruby Mountains, and East Humboldt Range. Folds shown in the Wood Hills are northwest-vergent overturned anticlines cored by small-displacement thrusts; these folds occupy a structural position in the hanging wall of the Independence thrust. The sillimanite-in isograd is for metapelite and the tremolite- and diopside-in isograds are for metacarbonate. Map is modified from Camilleri and Chamberlain (1997). Barometric data (solid squares) shown in the East Humboldt Range are from McGrew and Peters (1997) and in the Woods Hills from Hodges *et al.* (1992).

increase in metamorphic grade to upper amphibolite facies at deep structural levels. Metapelites underwent partial melting at the deepest levels (McGrew, 1992; Fig. 3a). Metamorphism is attributed largely to burial by the thrust wedge and consequent thermal relaxation (Camilleri and Chamberlain, 1997). U–Pb thermochronologic data suggest that peak metamorphism within the footwall is Late Cretaceous (~84 Ma) and that Barrovian metamorphism began at or after 154 Ma (Camilleri and Chamberlain, 1997). Figure 3(a) shows a cross section of the Windermere thrust at ~84 Ma. The age of the Windermere thrust and emplacement of the tectonic load depicted in Fig. 3(a) is only constrained to predate 84 Ma, the age of peak metamorphism. This inference is based on the logic that the load, inferred partly from barometric data, must have been emplaced prior to peak metamorphism that records high pressures. It is unknown, however, whether metamorphism began during or after loading.

Similarly, the time lag between the onset of loading (thrust faulting) and the inception of metamorphism is unknown.

Metamorphism of the footwall of the Windermere thrust was synchronous with development of a single foliation (S_1) and in places an elongation lineation (L_1). The development of foliation and lineation during metamorphism indicates that ductile flow accompanied prograde metamorphism. Ductile flow produced attenuation of stratigraphic units, and the amount of attenuation increases with increasing metamorphic grade (Camilleri, 1994; Fig. 3a).

Following peak metamorphism, the footwall of the Windermere thrust was deformed by the top-to-the-southeast Late Cretaceous Independence thrust (Camilleri and Chamberlain, 1997; Fig. 3b). The Independence thrust and a series of related minor back-folds and thrusts (Figs 2 & 3b) locally cut or fold S_1 . The Independence thrust is exposed in the Pequop

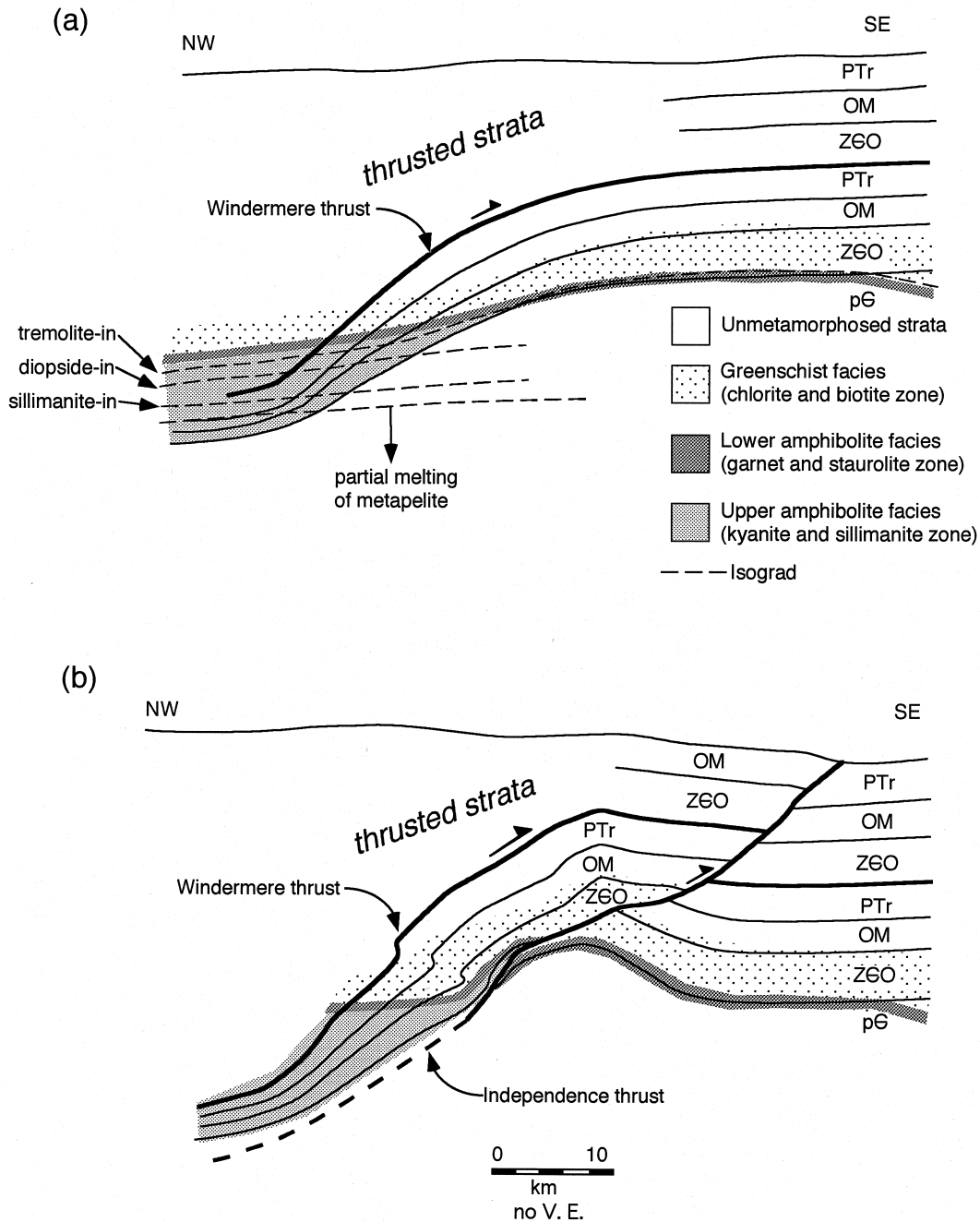


Fig. 3. (a) Cross-section of the footwall of the Windermere thrust showing distribution of metamorphic facies just prior to slip on the Independence thrust. (b) Cross-section of the Windermere and Independence thrusts prior to extension. Cross-sections are modified from Camilleri and Chamberlain (1997). pG = Proterozoic and Archean rocks; ZG0 = Proterozoic, Cambrian, and Ordovician strata; OM = Ordovician, Silurian, Devonian, and Mississippian strata; PTr = Pennsylvanian, Permian, and Triassic strata.

Mountains where it emplaces greenschist facies strata over unmetamorphosed strata (Fig. 2). Back folds in the hanging wall of the Independence thrust are exposed in the Wood Hills and Pequop Mountains (Fig. 2).

Following the development of the Independence thrust, the metamorphosed footwall of the Windermere thrust was exhumed by two phases of extension accommodated by west-rooted normal faulting (Camilleri and Chamberlain, 1997). The early phase of faulting is

inferred to be Late Cretaceous to possibly early Tertiary, synchronous with contraction in the frontal part of the Sevier orogen. This early phase of extension resulted in partial exhumation, decompression, and cooling of the metamorphosed strata (McGrew and Peters, 1997; Camilleri and Chamberlain, 1997). The younger phase of normal faulting is Tertiary and resulted in final exhumation of rocks in the footwall of the Windermere thrust as well as development of a

top-to-the-west-northwest normal-sense mylonitic shear zone (Fig. 2) that locally overprints S_1 (e.g. Snoke and Lush, 1984; Lister and Snoke, 1984; Snoke *et al.*, 1990; McGrew, 1992; Mueller and Snoke, 1993; Camilleri and Chamberlain, 1997; MacCready *et al.*, 1997). Presently, the structurally shallowest levels of the footwall of the Windermere thrust are exposed in the Pequop Mountains and Spruce Mountain and the deepest levels in the northwestern Wood Hills and East Humboldt Range. The prograde metamorphic foliation (S_1), which is the focus of this study, is well preserved in the central and southern Wood Hills, Windermere Hills, Pequop Mountains, and parts of Spruce Mountain, but is intensely overprinted by Tertiary ductile deformation in the Ruby Mountains and East Humboldt Range and in the northwestern corner of the Wood Hills.

MESOZOIC GEOMETRY AND DISTRIBUTION OF S_1 AND L_1

During the Mesozoic, the prograde metamorphic foliation within the footwall of the Windermere thrust is inferred to have ranged from horizontal to gently west-dipping, defining a broad zone of deformation with a gradational upper boundary (Fig. 4). Fabric is absent from structurally high unmetamorphosed rocks but increases in pervasiveness with depth away from the thrust (Fig. 4). Hence fabric development does not appear to have been related to slip along the Windermere thrust. There is no exposed lower boundary to the zone of deformation, thus it is not known what depth deformation extends to or if such a lower boundary existed. Moreover, because the hanging wall of the Windermere thrust was excised by normal faulting it is uncertain whether the metamorphic fabric

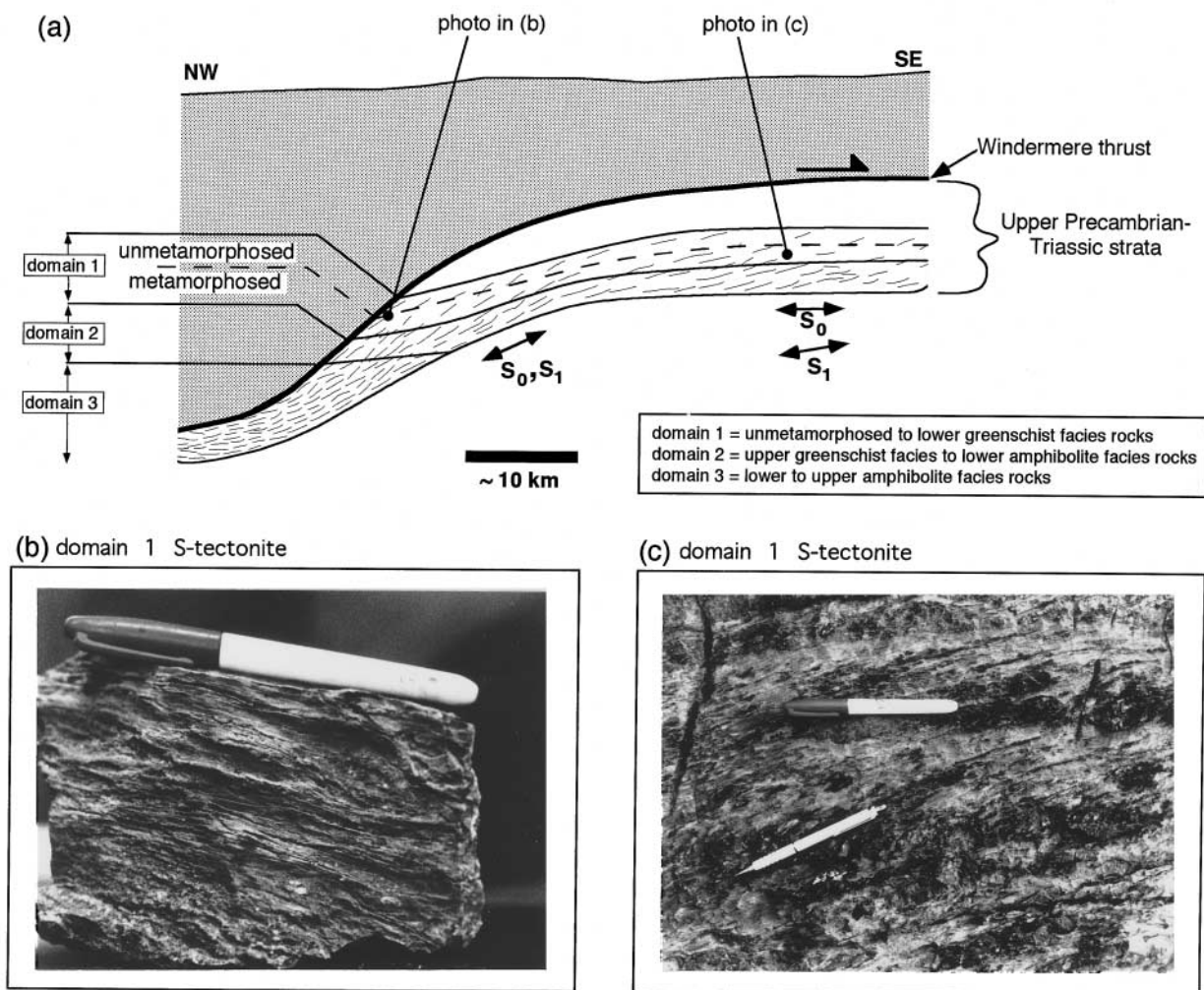


Fig. 4. (a) Cross-section of the hanging wall and footwall of the Windermere thrust illustrating geometry of foliation in the footwall, various fabric domains, and the approximate boundary between metamorphosed and unmetamorphosed rocks. Vertical scale is the same as the horizontal scale. (b) Photograph of bedding-parallel domain 1 cleavage in Permian limestone in the Windermere Hills area. Rock is an S tectonite. (c) Photograph of domain 1 cleavage in Ordovician limestone in the Pequop Mountains. Rock is an S tectonite. Large pen is parallel to bedding which is defined by resistant, silty layers. Note that the thin pen is inclined in the same direction as the cleavage but is at a slightly higher angle than the cleavage. The cross-section in (a) shows the structural positions of the photographs in (b) and (c).

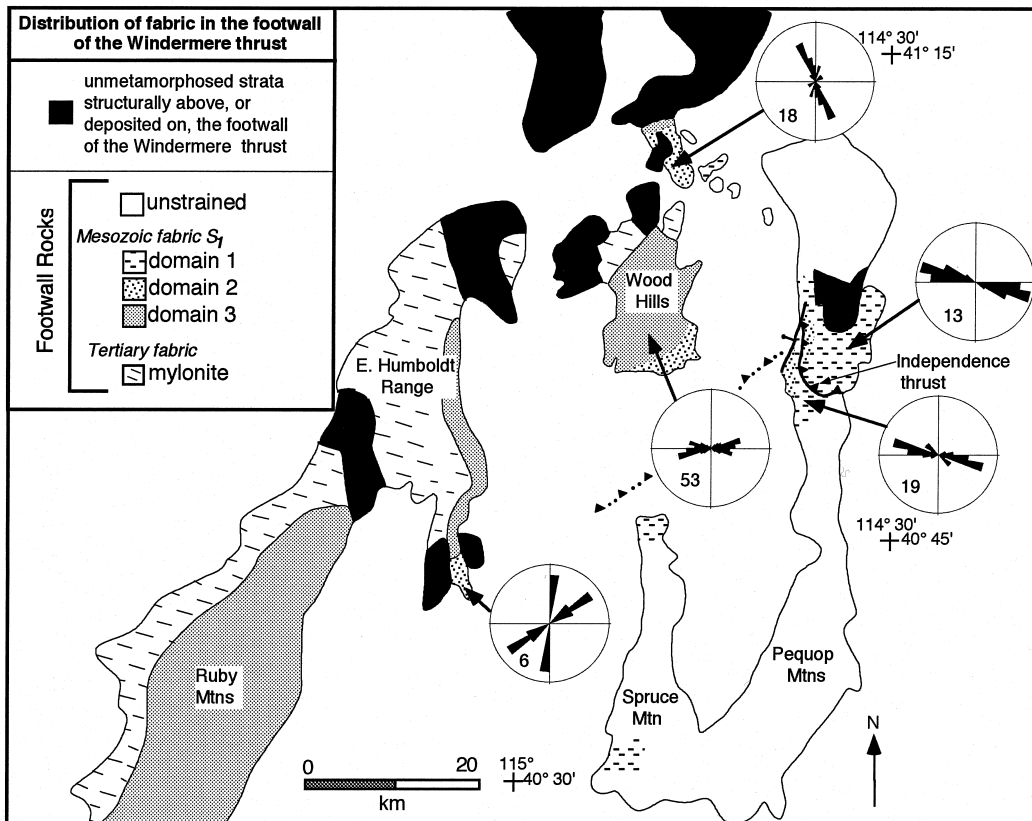


Fig. 5. Map depicting distribution of various Mesozoic fabric (S_1 , L_1) domains, and Rose diagrams of the trends of lineations (L_1) from upright stratigraphic sections. Lineation data are plotted bidirectionally. The perimeter of the diagram is 20%. Number of measurements is listed in the lower left-hand quadrant. All data were collected during this study, with the exception of lineation data from the Windermere Hills ($n = 18$) that was obtained from a geologic map by Mueller (1992). The distribution of Tertiary mylonitic rocks in the Ruby Mountains and East Humboldt Range is from Snoke and Lush (1984) and McGrew and Snee (1994).

extended laterally into structurally deep levels of the hanging wall of the thrust.

The fabric within the footwall of the Windermere thrust consists of S and $S > L$ tectonites. Foliation ranges from predominantly a solution cleavage in structurally high, very low-grade metamorphic rocks to a grain-shape foliation in structurally deeper, higher grade rocks. The foliation is predominantly parallel to bedding but locally is at a low angle to bedding (Fig. 4). Foliation is penetrative at deep structural levels and becomes increasingly partitioned (spaced) with decreasing metamorphic grade (Fig. 4). Elongation lineations are common in higher grade rocks and become scarce in lower grade rocks. Lineation is typically defined by mineral grain shape in monomineralic rocks and porphyroblast elongation in polymineralic rocks. The present trend of L_1 varies regionally (Fig. 5). In the southern Wood Hills L_1 trends west-southwest to west-northwest; in the Pequop Mountains it is west-northwest; in the Windermere Hills it is north-northwest; and in the southern East Humboldt Range it is north-northeast to northwest. It is unknown if the present regional variation in trends of lineations is original; however, there is no evidence that

lineations were significantly rotated after their formation.

CONVENTIONS AND METHODS

This study documents the distribution and geometry of metamorphic fabric (S_1 and L_1) and the style of strain that accompanied its development in the footwall of the Windermere thrust. Because S_1 is strongly overprinted in the East Humboldt Range–Ruby Mountains and in the northwestern corner of the Wood Hills by structures and fabrics formed during Tertiary extensional deformation, this study focuses on the metamorphosed Precambrian–Paleozoic strata in the footwall in the Wood Hills and Pequop Mountains, and to a much lesser extent rocks in Spruce Mountain, Windermere Hills and the southeastern East Humboldt Range. Assessment of the geometry and distribution of the metamorphic fabric was accomplished by detailed geologic mapping at a scale of 1:24,000 in the Wood Hills and Pequop Mountains and by reconnaissance observations in Spruce

Mountain, Windermere Hills, and the southeastern East Humboldt Range.

Two approaches were used to determine the type of strain that accompanied metamorphism. The first approach is a microstructural analysis of porphyroblasts in metacarbonate, metapelitic, and metapsammitic rocks. Common microstructural criteria were used to assess whether microstructures record mainly coaxial or non-coaxial strain (e.g. Ramsay and Huber, 1983; Simpson and Schmid, 1983; Lister and Snoke, 1984; Simpson, 1986). This method involved observations of fabric in thin sections oriented perpendicular to foliation and parallel and perpendicular to lineation as well as sections parallel to foliation. The second method is petrofabric analysis of preferred orientations of quartz *c*-axes in quartzites to determine if they record dominantly coaxial or non-coaxial deformation. The distribution of quartz *c*-axes has been shown empirically, theoretically, and experimentally to have a systematic relationship to (1) fabric axes within the rock, (2) the finite strain axes $X > Y > Z$, (3) type of finite strain, and (4) in some cases the strain path (e.g. Lister and Hobbs, 1980; Schmid and Casey, 1986; Law, 1990). For coaxial deformation, a flattening strain produces small circle girdles about the *Z* axis, whereas plane strain produces symmetric crossed girdles about the *ZY* plane. An increasing component of noncoaxial plane strain results in progressive kinking of crossed girdles and the loss of arms to a straight single girdle canted in the direction of simple shear. Quartz crystallographic *c*-axis orientations were obtained by standard methods on a universal stage. For samples with greater than 400 data points, orientations of *c*-axes were measured in two sections, both cut perpendicular to foliation but one parallel and one perpendicular to lineation. Data from the section cut perpendicular to lineation were rotated and added to data from the section cut parallel to lineation. In all cases rotated fabric patterns from the lineation-normal section yielded the same pattern as the lineation-parallel section. Orientations of *c*-axes for samples with less than 400 data points were obtained from a single section cut perpendicular to foliation and parallel to lineation. Quartz petrofabric analyses were particularly useful because the fabric developed in undeformed sedimentary rocks and hence lacked an inherited deformational fabric.

Samples investigated for assessment of strain during metamorphism were selected based on their lack of overprint by Tertiary mylonitization or overprint related to back folding in the hanging wall of the Independence thrust. Overprinting of S_1 by back folds in the hanging wall of the Independence thrust is sparse and generally restricted to the cores of folds and is manifest by axial-planar grain-shape foliation (S_2) and/or by crenulation or kinking of micas. Overprinting of S_1 in the Wood Hills by mylonitization is easily recognized by the presence of deformed,

commonly retrograded porphyroblasts or micas that sharply define asymmetric porphyroclasts. Thus, with the exception of one, samples selected for study contain only the S_1 prograde fabric, microstructurally have equilibrium textures, and lack retrogression.

Metamorphosed stratigraphic units in the footwall of the Windermere thrust are variably attenuated. Assessments of the amount (percent) of bulk attenuation of sedimentary units presented in this paper are derived from comparing the thickness of attenuated units with the same but undeformed, unmetamorphosed units in the Pequop Mountains and adjacent ranges (Camilleri, 1994).

FABRIC AND STRAIN TRANSITIONS

With increasing metamorphic grade and structural depth in the footwall of the Windermere thrust there are progressive changes in the dominant tectonite type, deformation mechanisms, pervasiveness of fabric elements, and amount of stratigraphic attenuation. These changes can be broadly grouped into domains that are approximately delimited by, and reflect changes in, metamorphic grade (cf. Figs 4 & 6). The footwall is divided into three domains, each representing progressively increasing metamorphic grade. Domain 1 contains unmetamorphosed and lower greenschist facies strata; domain 2 contains upper greenschist facies strata and some lower amphibolite facies strata; domain 3 contains upper amphibolite facies and some lower amphibolite facies strata. What follows are macroscopic and microscopic descriptions, quartz petrofabric data, and interpretations of the tectonites in each domain.

Domain 1: non-metamorphosed to lower greenschist facies

Domain 1 rocks comprise non-metamorphosed to lower greenschist facies strata exposed in the Pequop Mountains, Windermere Hills, and Spruce Mountain areas (Fig. 5). Foliation is parallel or at very low-angle to bedding in the Pequop Mountains but is parallel to bedding elsewhere. The *S* tectonites predominate within domain 1 rocks and *S-L* tectonites are scarce (Fig. 6). Foliation is partitioned into sparse, laterally discontinuous, zones a few centimeters to several meters thick. Foliated zones are separated by domains of undeformed, texturally unmetamorphosed rock a few meters to tens of meters thick (Figs 4 & 6). Domain 1 rocks also contain rare small-scale folds that are axial planar to S_1 . These folds generally have amplitudes of a few centimeters, are upright and lack vergence, although an easterly vergence was observed in two places. The amount of stratal attenuation within domain 1 stratigraphic units is negligible. The

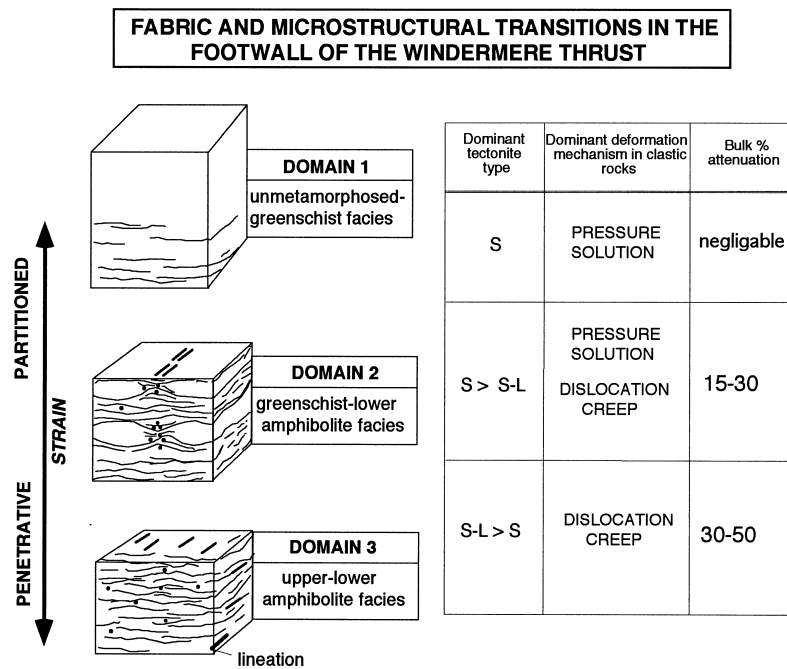


Fig. 6. Diagram summarizing fabric and microstructural transitions in the footwall of the Windermere thrust. Note that although the orientation of the lineation is portrayed as being parallel to the long axes of the swells, the geometry of the large-scale swells is unconstrained, and hence the orientation of the lineation relative to the geometry of the swells is uncertain.

following descriptions of domain 1 fabrics are from the Pequop Mountains.

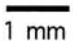
S_1 in metapelitic rocks is a typical phyllitic cleavage that is dominantly a product of pressure solution (Fig. 7a). Most quartz grains in pelitic rocks are internally undeformed; however, some grains exhibit minor subgrain development or incipient grain boundary migration where adjacent to another quartz grain. Foliation in calcareous rocks is a byproduct of both pressure solution and twin strain, and rigid objects such as crinoids or pyrite grains tend to have symmetric pressure shadows with straight quartz or calcite fibers. Lower greenschist facies quartzite contains no macroscopic foliation or lineation, but microscopic observation indicates that these rocks range from unstrained to moderately strained. In undeformed samples, quartz grains have quartz overgrowths and metamorphic micas occur only along detrital grain

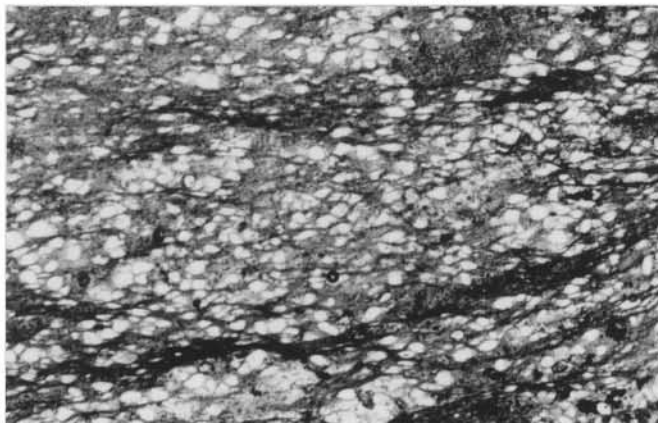
boundaries (Fig. 8a). In deformed samples, quartz grains are still surrounded by micas indicating preservation of original grain boundaries, however, at quartz-quartz grain boundaries minor subgrain development and grain boundary migration is evident (Fig. 8b). The most deformed quartzite has a weak microscopic grain-shape preferred orientation (Fig. 8b), however, the quartz *c*-axis patterns have little preferred orientation (Fig. 9).

In summary, pressure solution is the dominant deformation mechanism in polymineralic rocks, and recrystallization of quartz is minor within domain 1 rocks. The lack of asymmetric microstructure suggests that the rocks may have experienced dominantly coaxial deformation. The origin of sparse small scale folds is uncertain; they may be a product of shortening oblique to layering or may have formed in response to local components of non-coaxial or general shear.

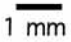
Fig. 7. Photomicrographs of domains 1 and 2 metapelites and metaconglomerate. Samples shown in (a) through (d) are from the Pequop Mountains and are in plain light, and sample in (e) is from the Windermere Hills and is in crossed polars. (a) Upper Ordovician chlorite-zone phyllite. Dark zones are solution seams that consist of sericite, chlorite, and opaque material. White grains are quartz. (b) Upper Cambrian biotite-zone schist showing biotite porphyroblasts (dark grains) with a static fabric. (c) Upper Cambrian biotite-zone schist. This foliation-parallel section shows biotite porphyroblasts (dark grains) defining the lineation in an *S-L* tectonite. Faint, thin light-colored bands within biotite crystals are cleavage splits filled with optically clear biotite and/or quartz. (d) Upper Cambrian biotite-zone schist. This foliation-parallel section shows randomly oriented biotite porphyroblasts (dark grains) in an *S* tectonite. (e) Greenschist facies Mississippian metaconglomerate. The section is perpendicular to foliation and parallel to lineation. The photograph shows two stretched chert clasts composed of very fine-grained quartz (center and bottom) and a rare undeformed quartz sandstone clast (top; sandstone clasts elsewhere in the same thin section are internally ductilely deformed). Note solution seams mantling clasts. The chert clast in the bottom of the photograph contains conjugate fractures in the center and a fracture that is approximately orthogonal to foliation and clast elongation on the extreme right at edge of photograph; fractures are filled with straight quartz fibers.

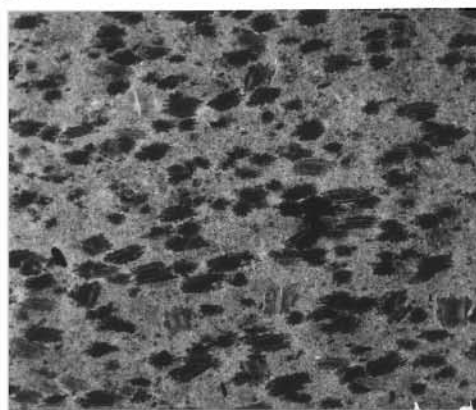
Domain 1 and 2 metapelite and metaconglomerate

(a) domain 1 S-tectonite 




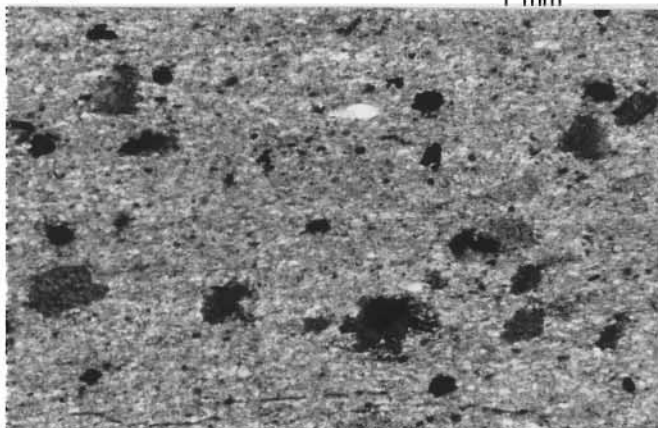
sample 23P: section perpendicular to foliation

(c) domain 2 S-L-tectonite 

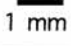


sample 132PC: section parallel to foliation

(b) domain 2 static fabric 

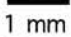


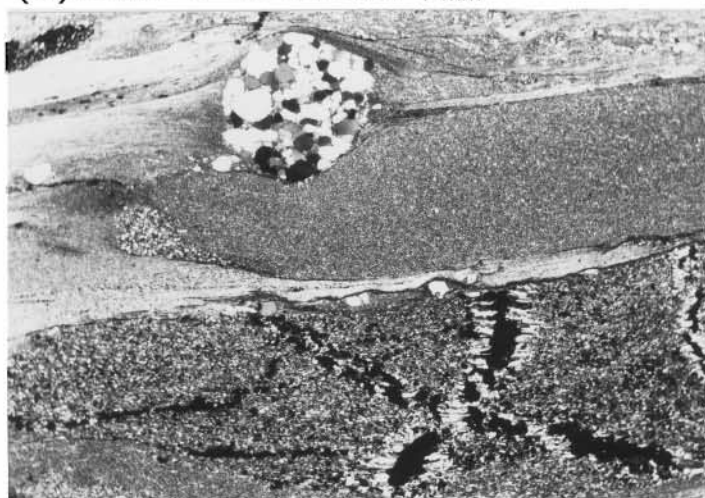
sample 38AP: section perpendicular to bedding

(d) domain 2 S-tectonite 



sample 81AP: section parallel to foliation

(e) domain 2 S-L-tectonite 



section perpendicular to foliation

Fig. 7(a)–(e)—Caption on previous page

Domain 1, 2, and 3 quartzite

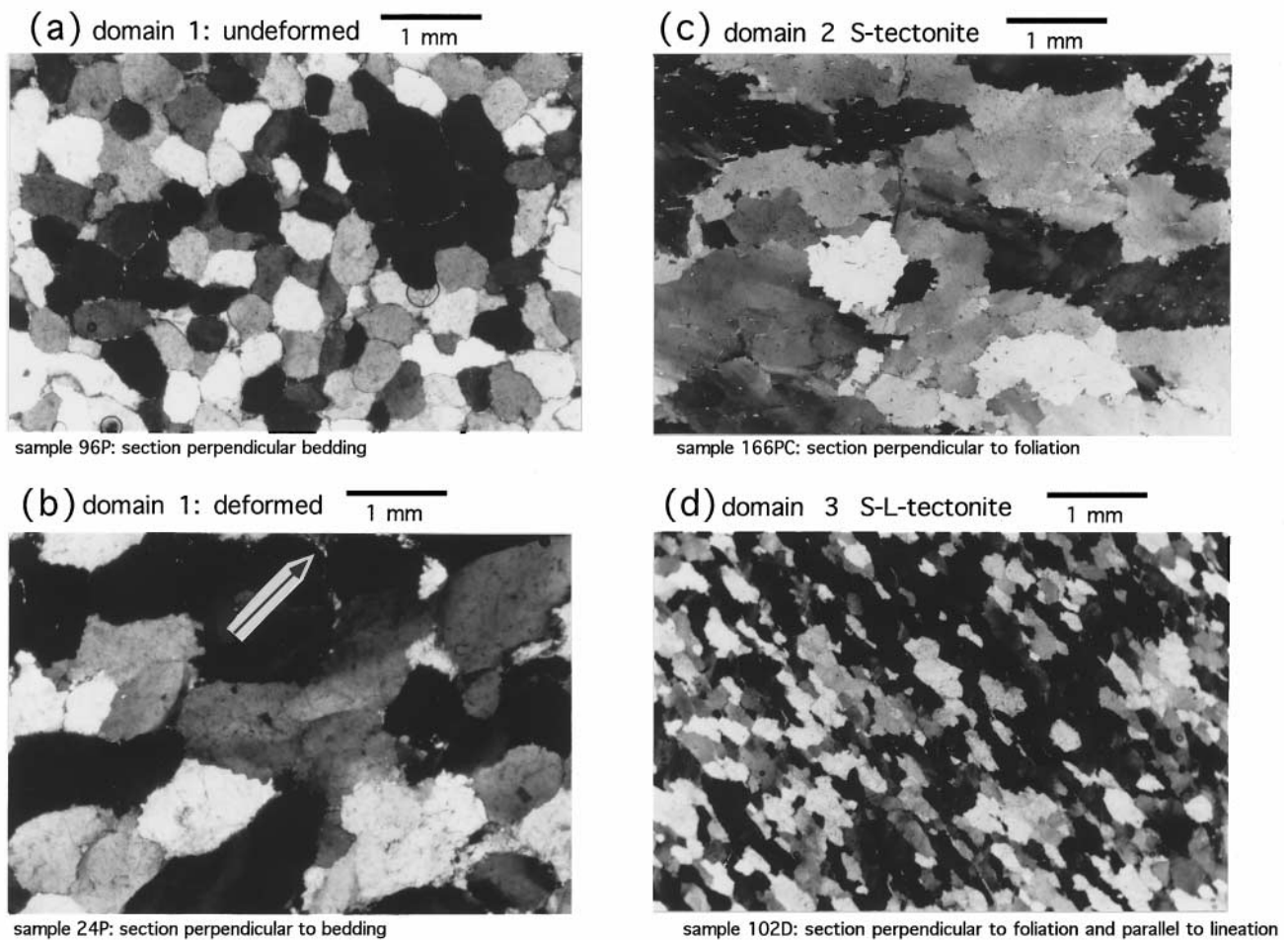


Fig. 8. Photomicrographs of domains 1, 2 and 3 quartzite in crossed polars. (a) Undeformed Ordovician chlorite-zone quartzite. Quartz grains have quartz overgrowths (not visible in photo), and are surrounded by metamorphic white micas (bright specks surrounding individual grains). (b) Deformed Ordovician chlorite-zone quartzite. Quartz grains are surrounded by tiny white micas (bright specks surrounding individual grains; arrow shows example). Serrate grain boundaries at quartz-quartz contacts provide evidence for minor grain boundary migration. (c) Cambrian garnet-zone quartzite. Elongate white specks within the grains are white micas. (d) Ordovician lower or upper amphibolite facies quartzite. Figures 9 and 13 show stereograms illustrating preferred orientations of crystallographic c -axes in the samples in (b & c) and (d), respectively.

Domain 2: upper greenschist to lower amphibolite facies

Domain 2 rocks range in metamorphic grade from upper greenschist to lower amphibolite facies and are exposed in the Pequop Mountains, Wood and Windermere Hills, and southernmost East Humboldt Range (Fig. 5). Foliation within domain 2 rocks appears to be predominantly parallel to bedding. In contrast to domain 1, domain 2 rocks record development of marked rheologic contrasts, which are manifest as gentle map-scale pinch-and-swell structure with wavelengths of several kilometers and amplitudes of a few tens of meters in addition to sparse outcrop-scale pinch-and-swell structure (Figs 6 & 10a). The three-dimensional geometry and orientation of large-scale pinches and swells are unknown because of the lack of areally extensive exposures of a third dimension.

Consequently, the orientation of lineation relative to these features is also unknown. However, in the few places where outcrop-scale pinch- and -swell structure was observed the lineations appear to be nearly parallel to the long axis of swells. The amount of attenuation of individual stratigraphic units within domain 2 varies dramatically because of the presence of large-scale pinch-and-swell structure. However, the amount of bulk attenuation for the section comprising domain 2 rocks is from ~15 to 30%.

Both S and $S-L$ tectonites are present in domain 2 rocks, but S tectonites are more abundant. In the thickest (swell) parts of stratigraphic units, the distribution of fabric resembles that described for domain 1 rocks wherein fabric is sparsely distributed and sedimentary textures and structures are preserved in undeformed or mildly deformed areas. In contrast, fabric is

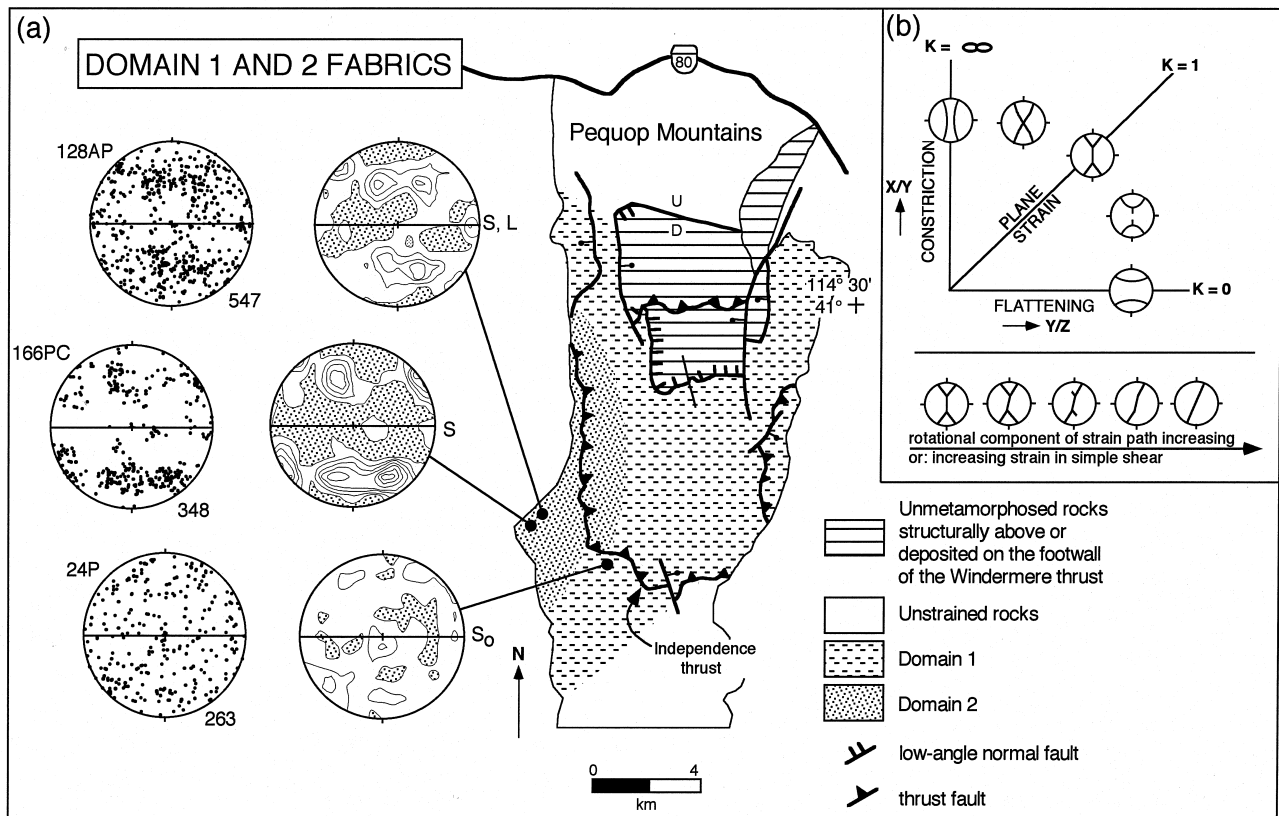


Fig. 9. (a) Quartz petrofabric data for domains 1 and 2 quartzite in the Pequot Mountains. The data, in this figure and Fig. 13, are plotted on equal-area nets and contoured by the Kamb method (Kamb, 1959) with a two-sigma contour interval. In each stereonet, foliation is vertical and lineation is horizontal; both are represented by a horizontal line transecting the center of the stereonet with the eastward direction on the right. Stratigraphic up is on the top of the stereonet. Locations for samples are given on 1:24,000 geologic maps in Camilleri (1994). (b) Geometry of quartz c -axis fabric skeletons expected for coaxial deformation (on the Flinn plot) and progressive non-coaxial deformation. On the stereogram X is horizontal, Y is perpendicular to the page, and Z is vertical. Part (b) is modified after Schmid and Casey (1986).

most penetrative in severely attenuated (pinch) parts, but even within these sections there are small low-strain domains where sedimentary structure is preserved. S tectonites predominate in both pinch and swell regions, but $S-L$ tectonites are more common in pinch, rather than in swell, regions (Fig. 6). In both pinch and swell regions there are sparse static metamorphic fabrics (Fig. 7b) where metamorphic minerals do not define a lineation or foliation. Rocks with static metamorphic fabrics have the same prograde mineral assemblages as tectonites whose metamorphic minerals define lineation and or foliation. This observation demonstrates the partitioning of strain during prograde metamorphism.

In metapsammitic and metapelitic $S-L$ tectonites, sparse garnet and more commonly biotite porphyroblasts typically have prolate shapes and define the mesoscopic lineation (Fig. 7c); in S -tectonites these minerals have more equant shapes (Fig. 7d). Most of the biotite crystals that define the lineation in $S-L$ tectonites are oriented such that their crystallographic c -axes lie in the plane of foliation and are nearly orthogonal to the lineation (Fig. 11a). The crystallographic

c -axes of the remainder of the biotite crystals are at low angles to lineation with even fewer perpendicular to foliation. In thin sections oriented parallel to lineation and perpendicular to foliation, biotite porphyroblasts whose c -axes are approximately normal to the plane of section (hereafter referred to as 'near-basal section') and porphyroblasts whose c -axes are at a low angle to lineation have different microstructures. Near-basal sections typically have smooth solution margins mantled by opaque material where they abut foliation and have highly irregular or serrate boundaries in symmetrical quartz-filled strain shadows, which suggests growth of biotite into the strain shadows and dissolution of biotite during deformation and metamorphism (Fig. 11b). Biotite crystals whose c -axes lie at a low angle to lineation exhibit 001-cleavage-parallel fractures (cleavage splits), filled with quartz and optically clear biotite that has grown across the split in crystallographic continuity with the original grain (Fig. 11c & d). Growth of biotite into cleavage splits and symmetrical pressure shadows in near-basal sections are indicative of coaxial deformation during metamorphism, wherein the shortening axis is perpen-

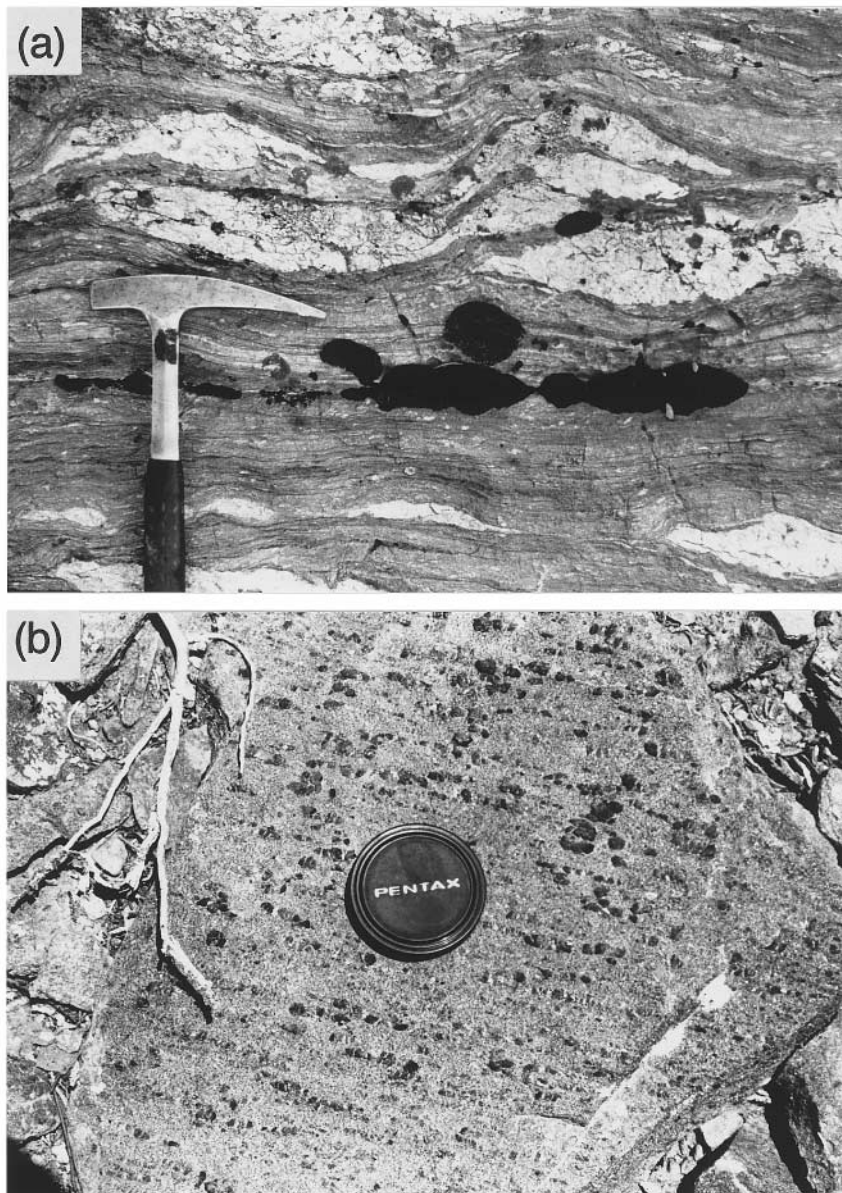


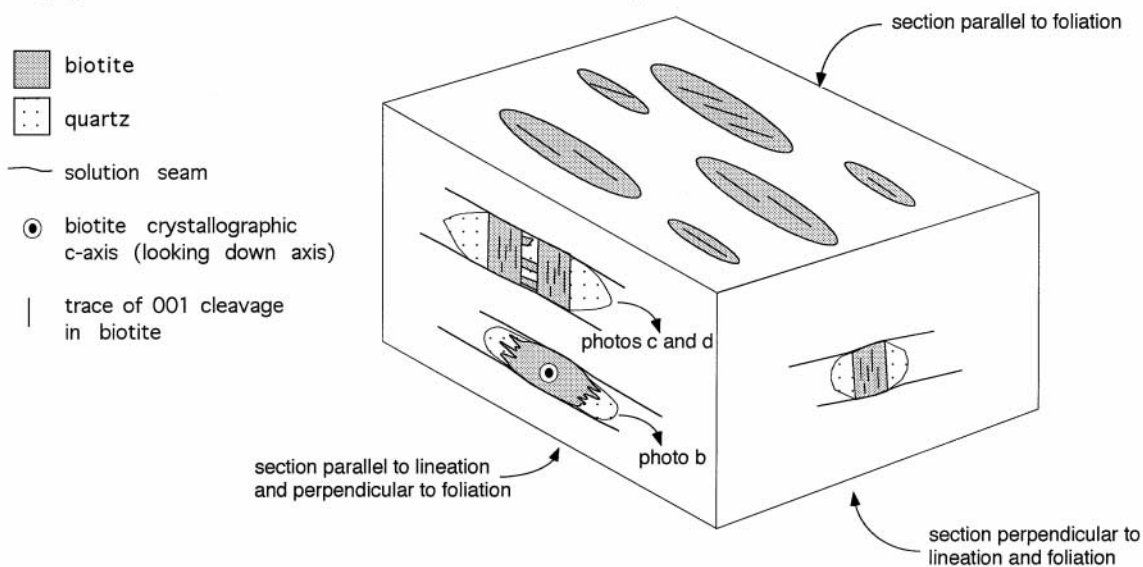
Fig. 10. (a) Photograph of pinch-and-swell structure in domain 2 Cambrian metacarbonates in the Pequop Mountains. View is looking obliquely down lineation. Boudins and surrounding material are composed of calcite; dark blobs in the center of the photograph are moss. (b) Photograph of biotite-zone domain 2 Cambrian metacarbonate in the Pequop Mountains. The rock is a hornblende–biotite–calcite marble. View is looking down on the foliation plane. The dark porphyroblasts are stretched hornblende crystals. Note the white zones in hornblende, which are lineation-normal fractures filled with calcite, quartz, and hornblende that has grown across the fracture.

dicular to foliation and the extension axis is parallel to lineation. The implication of the foregoing observations is that metapelitic and metapsammitic *S*–*L* tectonites are a result of dominantly coaxial deformation during metamorphism.

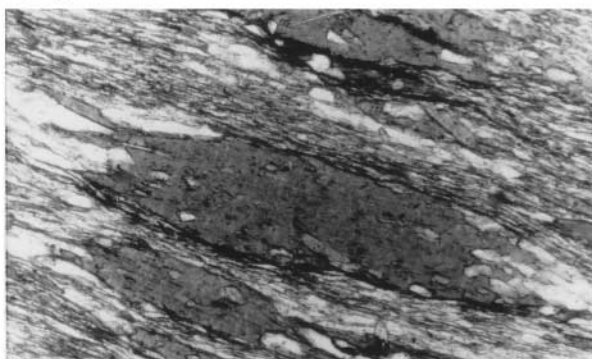
Sparse metaconglomerate in domain 2 also contains evidence for coaxial deformation. The conglomerates are composed mostly of chert clasts but also contain sparse quartz sandstone and limestone clasts. Flattened chert clasts define a rough foliation and in places a lineation. Pressure solution and recrystallization appear to be important deformation mechanisms responsible for clast elongation. Microscopically, pres-

sure solution is indicated by the presence of solution seams mantling clasts (Fig. 7e) and recrystallization of grains within chert clasts is indicated (with the gypsum plate inserted) by apparent crystallographic preferred orientation of fine grained quartz grains or by the presence of subgrains or evidence for grain boundary migration within larger quartz grains. Another less common mechanism that accommodated stretching of clasts was development of fractures that are approximately perpendicular to the long (*X*) axis of clasts or sparse intersecting conjugate fractures about the *Z* strain axis (Fig. 7e). The fractures are typically filled with undeformed, straight (approximately parallel to

(a) Biotite in domain 2 metapelitic S-L tectonites

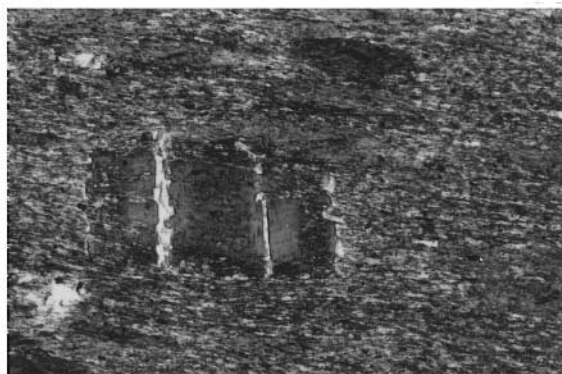


(b) domain 2 S-L-tectonite 1 mm



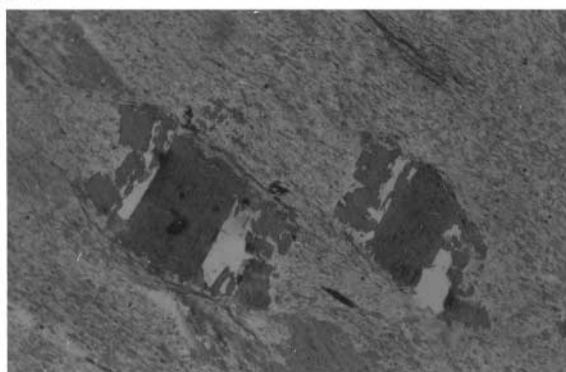
sample 2APP: section perpendicular to foliation and parallel to lineation

(c) domain 2 S-L-tectonite 1 mm



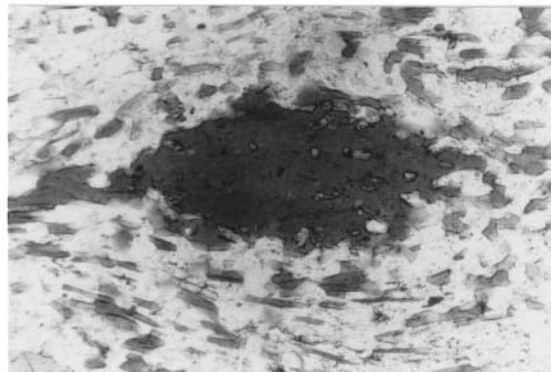
sample 132PCB: section perpendicular to foliation and parallel to lineation

(d) domain 2 S-L-tectonite 1 mm



sample 132PC: section perpendicular to foliation and parallel to lineation

(e) domain 3 S-L-tectonite 1 mm



sample 988-21B: section perpendicular to foliation and parallel to lineation

Fig. 11. (a) Sketch illustrating morphology of biotite in domain 2 metapelitic *S-L* tectonites. (b–e) are plain light photomicrographs of Upper to Middle Cambrian schist. (b–d) are in the biotite zone whereas (e) is in the kyanite zone. (b) A near-basal-section of a biotite porphyroblast that has grown into its own symmetric strain shadow. (c & d) Biotite porphyroblasts with cleavage splits and biotite that has grown into the split with crystallographic continuity with the porphyroblast. (e) Prolate near-basal-section of a biotite porphyroblast.

Domain 3 metacarbonate

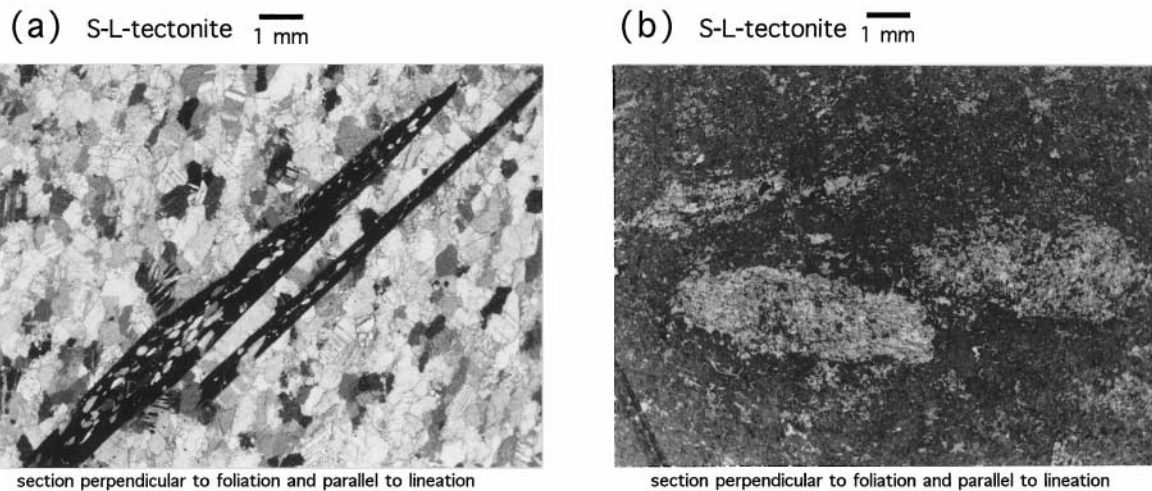


Fig. 12. Photomicrographs of domain 3 kyanite-zone metacarbonate in the Wood Hills. (a) Upper Cambrian dolomite marble with tremolite lineation. Crossed polars; the mineralogy is dolomite-quartz-tremolite. (b) Silurian calcite marble with diopside lineation. Plain light; the mineralogy is diopside-quartz-calcite. Calcite in this sample has been stained and therefore appears dark gray.

foliation) quartz fibers (Fig. 7e) indicating coaxial strain during extension of the clasts. Because most clasts yield evidence for internal plastic deformation, these extension fractures probably developed later in the strain history, possibly in response to strain hardening of the clast.

In metacarbonate rocks, recrystallization with and without twinning is the dominant deformation mechanism evident in *S* and *S-L* tectonites, whereas evidence for pressure solution is scarce. In impure marble *S-L* tectonites, hornblende, tremolite, and biotite or phlogopite define the lineation. Biotite or phlogopite porphyroblasts have prolate shapes and a preferred orientation similar to those discussed for metapelites and metapsammities; however, they notably lack pressure solution microstructure. Where hornblende defines the lineation it is boudinaged (Fig. 10b). Hornblende grains have irregular fractures perpendicular to lineation that are filled with quartz, calcite, and hornblende that has grown into the fracture [geometrically similar to Misch's (1969) paracrystalline boudinage]. These appear to be geometrically and kinematically similar to growth of biotite across cleavage splits in metapelites or metapsammities and imply a dominantly coaxial strain path during growth and extension of hornblende.

Quartzite within domain 2 rocks underwent extensive recrystallization indicating dislocation creep as a dominant deformation mechanism. Microstructures suggest that recrystallization was accomplished predominantly by grain boundary migration. Foliation within quartzite is defined by quartz grain shape and sparse micas, and micas are extensively included within quartz grains, hence no original grains are evident (Fig. 8c). Lineation, where present, is very weak and

defined by quartz grain shape. Quartz *c*-axes define small circles about the *Z* strain axis, indicating flattening strain and coaxial deformation (cf. Fig. 9a & b), which is consistent with microstructures from other rock types.

In summary, pressure solution and dislocation creep are important deformation mechanisms within domain 2 rocks. Quartz petrofabric data, and the lack of asymmetric microstructure in all rock types, suggest dominantly coaxial deformation during fabric development and metamorphism. The presence of static prograde metamorphic fabric in undeformed areas reflects the partitioning of strain during metamorphism.

Domain 3: lower to upper amphibolite facies

Domain 3 rocks discussed here consist of lower to upper amphibolite facies strata exposed in the Wood Hills. Both *S-L* and *S* tectonites are present within domain 3, but *S-L* tectonites are more abundant. In this domain, bedding is parallel to foliation, fabric elements are more penetratively distributed, and static fabrics are scarce. In a few places, in the higher grade part of the Wood Hills, domain 3 rocks contain small outcrop-scale isoclinal folds. These folds, although sparse, are interpreted to have formed synchronous with metamorphism because they do not deform the metamorphic fabric and lie within the plane of foliation. Stratigraphic units in domain 3 tend to have a more uniform, albeit attenuated, thickness suggesting less pronounced pinch-and-swell structure and a reduction in the rheological contrasts between layers. The amount of stratigraphic attenuation is from ~30 to 50%. The dominant deformation mechanism for all

rock types is dislocation creep and microstructural evidence for pressure solution is lacking.

Most of the metapelites and metapsammites are *S-L* tectonites. Feldspar, biotite, and less commonly staurolite, porphyroblasts have prolate shapes, define the lineation, and lack asymmetric microstructure (Fig. 11e). These porphyroblasts are geometrically like domain 2 porphyroblasts, but lack evidence for pressure solution (compare microstructure in Fig. 11b & e).

Metacarbonates commonly have a well developed crystallographic preferred orientation as well as grain-shape fabric, but there are domains where rocks contain a more static fabric and carbonate grains and porphyroblasts are randomly oriented. Lineation within metacarbonate is defined by calcite and dolomite grain shape and/or by tremolite and diopside porphyroblasts that lack asymmetric microstructure (Fig. 12).

All domain 3 quartzites have undergone extensive recrystallization. Like domain 2 quartzite, quartz grains include micas and no original grains are evident (Fig. 8d). Microstructures suggest recrystallization in *S-L* tectonites was accomplished by both subgrain rotation and grain boundary migration, however, grain boundary migration appears to be a predominant mechanism in *S*-tectonites. Several Ordovician quartzite samples were selected for analysis of crystallographic preferred orientation of quartz *c*-axes (Fig. 13).

Samples 4D, 5D, and 102D, from the lower grade part of the Wood Hills (Fig. 13), are *S-L* tectonites that have a weak to moderate grain-shape lineation, which is reflected by the slightly greater degree of grain elongation in lineation-parallel sections than in lineation-normal sections. These samples yield crossed girdle patterns indicative of plane strain (cf. Figs 13 & 9b). Samples 102D and 5D are symmetric and imply coaxial strain (Fig. 13). In contrast, Sample 4D shows a distinct asymmetry suggesting a component of top-to-the-SE shear. Sample 1088-6 is an *S*-tectonite with scarce diopside porphyroblasts that lie in the foliation plane but do not define a lineation. The *c*-axis pattern in this sample forms small circles about the *Z* axis and is interpreted to indicate coaxial flattening strain (Fig. 13), which is consistent with the absence of lineation in the rock. Patterns for samples 86C and 62C show slightly uneven density distributions but are consistent with coaxial deformation. Sample 62C shows a broadly symmetric crossed girdle pattern suggesting plane strain whereas sample 86C has a weak *Y* maximum and is more similar to a pattern transitional between coaxial flattening ($k = 0$) and plane strain

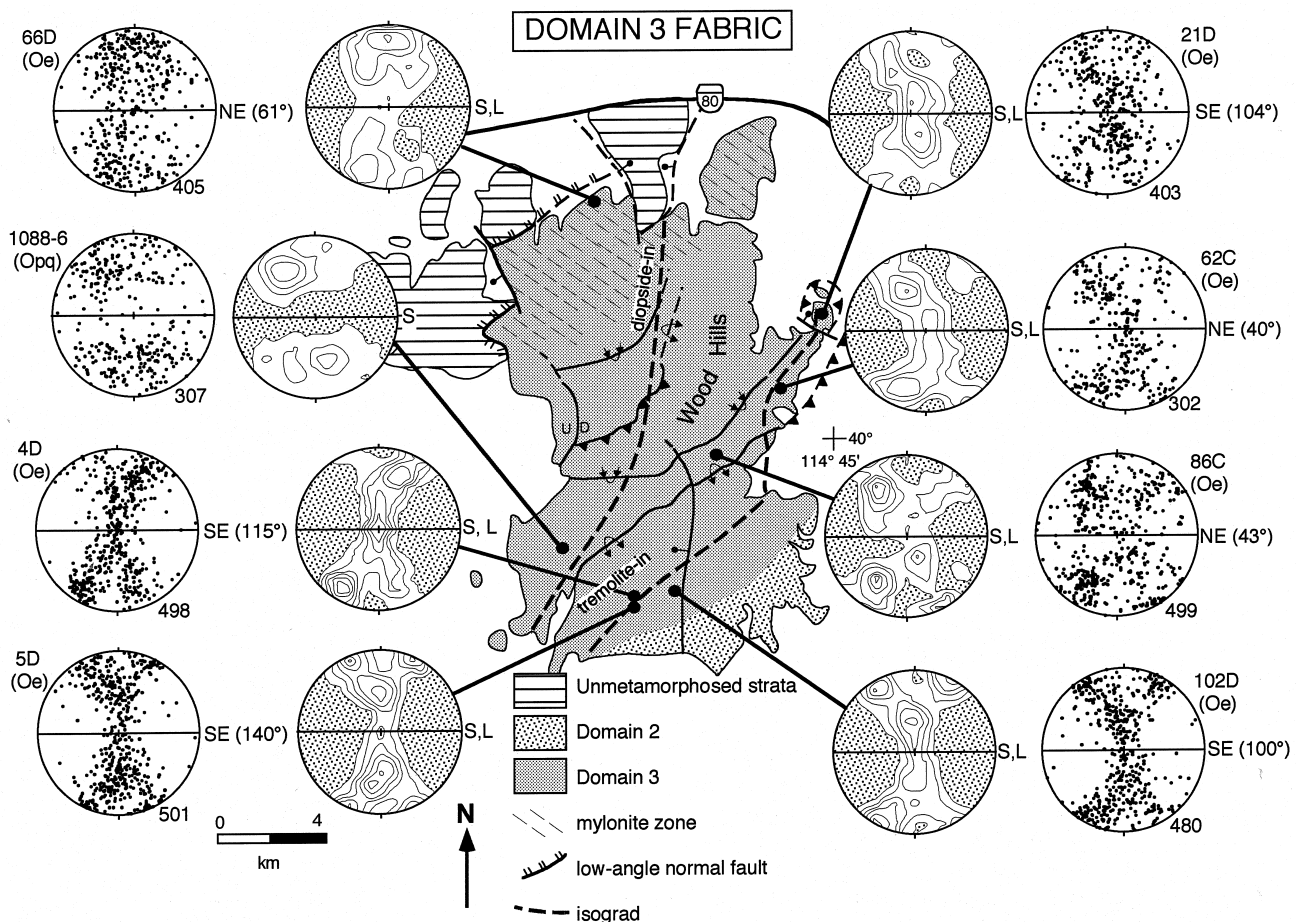


Fig. 13. Quartz petrofabric data for domain 3 quartzite in the Wood Hills.

($k = 1$; cf. Figs 13 & 9b). Sample 66D is of higher metamorphic grade than the other samples and is within the mylonite zone but is from an area where S_1 is not overprinted by mylonitization. The c -axis pattern (Fig. 13) in this sample is unlike the classic patterns developed in other samples, but its symmetry suggests dominantly coaxial deformation. Sample 21D is from a tightly appressed core of a minor northwest-vergent overturned anticline, which folds S_1 , in the hanging wall of a minor thrust fault associated with the southernmost anticline in the Wood Hills (Fig. 13). This sample differs from the former because micas are crenulated and hence were deformed during fold development. Because of the structural position of this sample and the fact that the micas are deformed, the resultant c -axis pattern probably reflects strain imposed by fold development. The c -axis pattern is asymmetric (Fig. 13) and suggests a component of top-to-the-northwest shear, which probably reflects flow in the core of the fold and is consistent with the northwest vergence of the fold.

With the exception of sample 21D, the predominantly symmetric quartz lattice-preferred orientation data indicate a strong component of coaxial deformation (cf. Figs 9b & 13) during peak metamorphism, consistent with the lack of asymmetric microstructure in porphyroblasts or micas within all rock types. However, at least locally the data, as exemplified by sample 4D, do indicate some component of non-coaxial flow. Moreover, the presence of rare outcrop-scale isoclinal folds within S_1 in some of the highest grade rocks probably reflects local components of non-coaxial flow. Overall, however, the data from domain 3 rocks suggest mainly coaxial deformation with plane strain dominant over flattening, which is supported by the greater abundance of S - L tectonites.

Summary: partitioning of fabric and style of strain

From the foregoing observations of rocks in domains 1, 2, and 3, the following five inferences can be made about the character of deformation during prograde metamorphism of the footwall of the Windermere thrust (see also Fig. 6):

1. Fabric is highly partitioned in weakly metamorphosed to lower greenschist facies rocks and becomes increasingly penetrative with increasing metamorphic grade.
2. The partitioning of strain during metamorphism resulted in development of sparse static metamorphic fabrics in undeformed areas surrounded by tectonites. Furthermore, the partitioning of the type of strain (flattening [$k = 0$] to plane strain [$k = 1$]) resulted in production of a wide range of tectonites from S only to those with varying degrees of lineation development.

3. S tectonites predominate in non-metamorphosed to lower amphibolite facies rocks and S - L tectonites predominate in upper amphibolite facies rocks.
4. The overall dominant type of strain recorded by the metamorphic rocks is coaxial, but style of strain appears to be partitioned from dominantly flattening strain in greenschist and lower amphibolite facies rocks to plane strain in upper amphibolite facies rocks.
5. The amount of bulk attenuation, which is a measure of the amount of strain, ranges from negligible in unmetamorphosed to lower greenschist facies rocks to ~50% in upper amphibolite facies rocks. Therefore, the amount of bulk attenuation increases with metamorphic grade.

TECTONIC AND STRUCTURAL INTERPRETATION

The footwall of the Windermere thrust contains a single prograde metamorphic fabric, and microstructural and quartz petrofabric data suggest that mainly coaxial deformation accompanied the peak of metamorphism. Although the footwall contains evidence for sparse local components of non-coaxial flow, the lack of evidence of a regionally pervasive and significant component of non-coaxial flow suggests that attenuation of stratigraphic units was accomplished predominantly by coaxial deformation and that the strain path during metamorphism may have been largely coaxial. Development of the prograde metamorphic fabric and attenuation of the footwall appears to be an intrinsic consequence of heating of the footwall during and or following loading wherein the amount of attenuation is a function of decreasing 'viscosity' of the footwall concomitant with increasing metamorphic grade (Fig. 4). The evolution of strain and development of a gentle westward dip of the metamorphic fabric (Fig. 4) in the footwall of the Windermere thrust can be explained in terms of two processes: (1) footwalls of thrust sheets flex under the imposed hanging wall load, and (2) over time, thermal relaxation decreases the strength of footwall rocks. Initial loading of the footwall probably produced a largely elastic flexure with little permanent footwall strain. With relative upward migration of isotherms through the footwall and loss of rock strength, deep structural levels lose their flexural strength and collapse by plastic extension.

Tectonic model

Figure 14 is a schematic model that illustrates the process of loading, flexure, and attenuation. Although

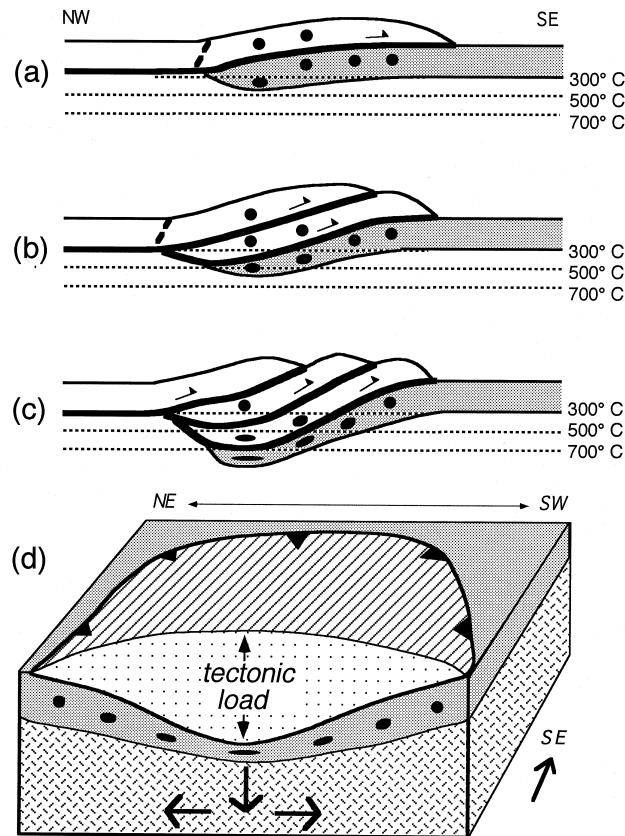


Fig. 14. Schematic model depicting the flexural and extensional evolution of a thrust footwall. (a–c) are transport-parallel cross-sections. The block diagram in (d) highlights a cross-section perpendicular to the thrust transport direction at the same stage represented by the transport-parallel cross-section shown in (c).

it is unknown whether the inception of prograde metamorphism in the footwall of the Windermere thrust took place after loading or during loading, for simplicity the model assumes metamorphism began during loading. This model shows a footwall, which schematically represents the footwall of the Windermere thrust, that is progressively loaded by three thrust sheets (Fig. 14). Because the Windermere thrust is likely to have been a localized feature along the bend in the Paleozoic shelf-slope margin in the Sevier hinterland, the model depicts a localized (Fig. 14d), rather than a long linear load. Implicit in this model is that the principal stresses rotate from sigma-one being horizontal in the upper crust, which is regionally in a state of contraction, to sigma-one being vertical in the middle to lower crust, which is undergoing extension in response to the developing load. For simplicity, in the model it is assumed that isotherms are fixed and that during loading and thermal relaxation the footwall passes through the isotherms without depressing them. Because fabric development is first observed at the transition between metamorphosed and unmetamorphosed rock, it is assumed that initial extension and fabric development begins at a temperature of $\sim 300^{\circ}\text{C}$, i.e. lower greenschist facies. Strain ellipses are also shown for various positions in the thrust sheets

(Fig. 14), and their departure from spherical is meant to show schematically the amount of attenuation with increasing temperature. In Fig. 14(a), initial loading results in flexure of the footwall. The flexure is largely elastic, however, the lowermost part of the footwall is depressed through the 300°C isotherm. Thermal weakening below the 300°C isotherm induces initial extension and development of a weak, partitioned flattening fabric. In Fig. 14(b) an additional load is emplaced resulting in relative upward migration of isotherms and thermal weakening and stretching of a much greater portion of the footwall. In Fig. 14(c) this process is continued with emplacement of yet another thrust sheet. The additional load induces more pronounced attenuation in the footwall as well as stretching of the deepest part of the next higher thrust sheet. Extreme loading would ultimately result in a stack of attenuated thrust sheets that contain a layer-parallel prograde metamorphic fabric that records bulk coaxial deformation.

The model suggests some of the mechanisms by which the upper portions of footwalls of thick thrust sheets could accommodate attainment of isostatic equilibrium. Flexure at upper structural levels accompanied by plastic extension at deeper levels may facilitate relative sinking of the load and lowering of topography.

This process suggests that extension during metamorphism assists to laterally spread and increase the thickness of a crustal root as well as to minimize topography.

Although the model in Fig. 14(a–c) is two-dimensional it is important to emphasize that on a regional basis the strain in the footwall of the Windermere thrust is three-dimensional. For example, the preponderance of flattening strain, as manifest by *S* tectonites, indicates stretching in all directions. Furthermore, the present regionally variable trends of lineations suggest that principle extension directions may have been partitioned into domains (Fig. 5). The foregoing observations suggest that extension occurred parallel, obliquely, and even perpendicular to the plane of the section as shown in Figs 4 and 14(c) (see Fig. 14d for inferred footwall geometry in a cross-section perpendicular to thrust transport direction).

Comments on strain partitioning

The fabric domains in the footwall of the Windermere thrust record different degrees of the spatial partitioning of strain as well as the partitioning of the style of strain. The metamorphic-strain transitions preserved in domains 1 and 2, respectively, are interpreted to reflect stages in the progressive evolution of strain during metamorphism that ultimately culminated in the development of penetrative fabrics in domain 3. Overall, the observed partitioning of strain is probably an inherent consequence of imposing dominantly coaxial deformation on a sedimentary sequence with layers of varying competency. Competency contrasts exist vertically between units and laterally within units due to lithologic variability in the Paleozoic section. The highly partitioned *S* tectonite fabric in domain 1 rocks probably developed locally around more competent zones. An analogy to this at the microscopic scale is the development of solution seams around rigid (competent) quartz or feldspar grains in low-grade metapsammite. In domain 2, competency contrasts resulted in development of gentle, map-scale pinch-and-swell structure wherein much of the *S*-tectonites are concentrated around the little-deformed swells and penetrative *S*–*L*, as well as *S*, tectonites are concentrated in the pinch domains. The concentration of *S*–*L* tectonites in pinch areas in domain 2 rocks and the greater abundance of *S*–*L* than *S* tectonites in domain 3 rocks implies that with increasing strain (i.e. greater attenuation), the style of strain becomes more partitioned between plane strain and flattening, probably to maintain strain compatibility.

Comparisons with other metamorphic terranes

Dominantly coaxial deformation, or components of coaxial deformation, during metamorphism are begin-

ning to be recognized as an important component of the early evolution of polydeformed internal zones of contractional orogens (e.g. Law *et al.*, 1984; Wells and Allmendinger, 1990; Northrup, 1996; Wells, 1997). Two metamorphic terranes, the Black Pine Mountains along the Utah–Idaho border (Fig. 1) and the Moine thrust zone in Scotland, bear noteworthy structural resemblance to fabrics in the footwall of the Windermere thrust albeit they do not contain a complete spectrum of metamorphic fabrics and grades within a single thrust sheet or footwall. Cretaceous coaxial fabrics similar to those described herein for domain 2 rocks occur elsewhere in the Sevier hinterland in the Black Pine Mountains (Wells and Allmendinger, 1990). In low- to medium-grade metamorphic rocks in the Black Pine Mountains, Wells and Allmendinger (1990) documented as much as 160% bedding-parallel extension of stratigraphic units accommodated by dominantly coaxial deformation. Although the superposition of polyphase extensional and contractional structures on rocks in the Black Pine Mountains (Wells and Allmendinger, 1990) has not permitted a large-scale structural reconstruction of these fabrics at the time of their formation, on the basis of similarity, they may have once formed part of a zone of deformation like that depicted in Fig. 5 for the footwall of the Windermere thrust. In the Moine thrust zone, Law *et al.* (1984) utilized crystallographic preferred orientations of quartz *c*-axes to document strain partitioning in very low-grade metamorphic rocks. Their quartz petrofabric data indicate non-coaxial strain in proximity of thrusts and predominantly coaxial strain in the central and upper parts of thrust sheets. Coaxial deformation included components of flattening and plane strain, similar to that observed in the footwall of the Windermere thrust. Law *et al.*'s (1984) coaxial quartz petrofabric data are similar to those shown in Figs 9 and 13 for domain 2 and 3 quartzite, however, rocks in the Moine thrust zone probably represent a metamorphic grade more consistent with domain 1 rocks. Thus, in contrast to the very low grade rocks in the Moine thrust zone, quartzites of similar metamorphic grade in the footwall of the Windermere thrust did not develop strong crystallographic preferred orientations or a macroscopic fabric. Law *et al.* (1984) suggested that coaxial deformation within thrust sheets could be related to loading, roughly similar to the interpretation for the footwall of the Windermere thrust, or related to spreading along a thrust ramp. In summary, these examples as well as the footwall of the Windermere thrust, serve to illustrate that partitioned coaxial flattening and plane strain may be an important aspect of the strain path of metamorphosed thrust footwalls.

IMPLICATIONS

Documentation of polyphase fabrics and structures is a common aspect of assessing the strain history of dynamically metamorphosed internal zones. Unfortunately, the common occurrence of intense polyphase deformation and lack of preservation or exposure of complete upper to middle crustal cross sections in high-grade parts of internal zones often makes it difficult to reconstruct rocks and fabrics for a particular phase of deformation. Thus, the large-scale structural position, distribution, and type(s) of strain developed during a certain fabric forming event are commonly not discernible, in particular with respect to early prograde metamorphic fabrics. The footwall of the Windermere thrust is a rare exposure of a nearly complete sequence of prograde metamorphic fabrics formed in response to tectonic burial. Furthermore, the footwall of the Windermere thrust serves as a generic model for the large-scale distribution and type of strain that may accompany metamorphism of sedimentary footwalls of thick thrust sheets. Whether or not the prograde fabric architecture observed in the footwall of the Windermere thrust is broadly applicable to footwalls in other contractional orogens remains to be tested, however, strain patterns would probably vary in areas where magmatism plays a significant role in heterogeneous heat distribution within a footwall or for thrusts that develop in crustal sections with complex lithologic or rheological properties. In addition, the rate of loading, stretching, and thermal relaxation could be a factor in the nature of attenuation of the footwall. For example, it is also possible to facilitate footwall attenuation by a bulk pure shear that involves an array of ductile, conjugate normal-sense shear zones that are at a low-angle to bedding.

In summary, the data and interpretations presented in this paper have important implications for the nature of Barrovian metamorphism and attendant regional metamorphic fabrics within overthrust sequences in internal zones of contractional orogenic belts. The results of this study imply that, during thermal relaxation and prograde metamorphism, sedimentary footwalls of thick thrust sheets undergo dominantly coaxial deformation that produces a bedding-parallel or near bedding-parallel foliation. This process is induced by thermal weakening of the footwall under a sufficient hanging wall load, and ultimately results in collapse, or attenuation, of the footwall. The distribution and type of strain in the footwall is heterogeneous on a large scale. Partitioned, predominantly flattening strain at low-temperatures in upper structural levels gradually gives way to a mix of increasingly penetrative plane strain and flattening at hotter, deeper structural levels.

Acknowledgements—This work was funded by the Geological Society of America, American Association of Petroleum Geologists, Sigma

Xi, Wyoming Geological Association, Shell Oil Company, U.S. Geological Survey, and National Science Foundation grant EAR 87-07435 (awarded to A. W. Snoke). Support for the production of this manuscript came from an Austin Peay State University Tower Grant. Thanks to Al McGrew, who reviewed an earlier version of this paper, and to JSG reviewers Margi Rusmore and Michael Wells and Associate Editor Peter Hudleston whose comments and suggestions greatly helped improve the final version of this manuscript. This work has benefited from discussions with B. Ron Frost, Allen McGrew, Tyler MacCready, Arthur Snoke, Michael Wells, David M. Miller, and Karl Mueller. Thanks also go to Karl Mueller for loan of thin sections from the Windermere Hills.

REFERENCES

- Camilleri, P. A. and Chamberlain, K. R. (1997) Mesozoic tectonics and metamorphism in the Wood Hills and Pequop Mountains region, northeast Nevada: implications for the architecture and evolution of the Sevier orogen. *Geological Society of America Bulletin* **109**, 74–94.
- Camilleri, P. A. (1994) Mesozoic and Cenozoic tectonic and metamorphic evolution of the Wood Hills and Pequop Mountains, Elko County, Nevada. Unpublished Ph.D. thesis. University of Wyoming.
- Camilleri, P. A., Miller, D. M., Snoke, A. W. and Wells, M. E. (1992) Structure and fabric of metamorphic terrains in the north-eastern Great Basin: Implications for Mesozoic crustal shortening and extension. In *Field guide to geologic excursions in Utah and adjacent areas of Nevada, Idaho, and Wyoming*, ed. J. R. Wilson, pp. 19–58. Utah Geological Survey Miscellaneous Publication, **92**.
- England, P. C. and Thompson, A. B. (1984) Pressure–temperature–time paths of regional metamorphism I. Heat transfer during the evolution of regions of thickened continental crust. *Journal of Petrology* **25**, 894–928.
- Hodges, K. V., Snoke, A. W. and Hurlow, H. A. (1992) Thermal evolution of a portion of the Sevier hinterland: the northern Ruby Mountains–East Humboldt Range and Wood Hills, northeastern Nevada. *Tectonics* **11**, 154–164.
- Kamb, W. B. (1959) Petrofabric observations from Blue Glacier, Washington, in relation to theory and experiment. *Journal of Geophysical Research* **64**, 1908–1909.
- Law, R. D. (1990) Crystallographic fabrics: a selective review of their application to research in structural geology. In *Deformation mechanisms, rheology and tectonics*, eds R. J. Knipe and E. H. Rutter, pp. 335–352. Geological Society Special Publication, **54**.
- Law, R. D., Knipe, R. J. and Dyan, H. (1984) Strain path partitioning within thrust sheets: Microstructural and petrofabric evidence from the Moine thrust zone at Loch Eriboll, northwest Scotland. *Journal of Structural Geology* **6**, 477–497.
- Lister, G. S. and Snoke, A. W. (1984) S–C mylonites. *Journal of Structural Geology* **6**, 617–638.
- Lister, G. S. and Hobbs, B. E. (1980) The simulation of fabric development during plastic deformation and its application to quartzite: the influence of deformation history. *Journal of Structural Geology* **2**, 335–370.
- MacCready, T., Snoke, A. W., Wright, J. E. and Howard, K. A. (1997) Mid-crustal flow during Tertiary extension in the Ruby Mountains core complex, Nevada. *Geological Society of America Bulletin* **109**, 1576–1594.
- McGrew, A. J. (1992) Tectonic evolution of the northern East Humboldt Range, Elko County, Nevada. Unpublished Ph.D. thesis. University of Wyoming.
- McGrew, A. J. and Peters, M. T. (1997) Petrogenesis and thermal evolution of deep continental crust: the record from the East Humboldt Range, Nevada. In *Proterozoic to Recent stratigraphy, tectonics and volcanology, Utah, Nevada, southern Idaho and central Mexico*, eds P. K. Link and B. J. Kowallis, pp. 270–275. Brigham Young University Geology Studies, **42**.
- McGrew, A. J. and Snee, L. W. (1994) $^{40}\text{Ar}/^{39}\text{Ar}$ thermochronologic constraints on the tectonothermal evolution of the northern East Humboldt Range metamorphic core complex. *Tectonophysics* **238**, 425–450.
- Miller, D. M. and Hoisch, T. D. (1992) Mesozoic structure, metamorphism, and magmatism in the Pilot and Toano ranges. In *Field guide to geologic excursions in Utah and adjacent areas of*

- Nevada, Idaho, and Wyoming*, ed. J. R. Wilson, pp. 79–92. Utah Geological Survey Miscellaneous Publication, **92**.
- Miller, D. M., Repetski, J. E. and Harris, A. G. (1991) East-trending Paleozoic continental margin near Wendover, Utah. In *Society of Economic Paleontologists and Mineralogists, Pacific Section*, eds J. D. Cooper and C. H. Stevens, **67**, pp. 439–461.
- Misch, P. (1969) Paracrystalline boudinage of zoned grains and other criteria for synkinematic growth of metamorphic minerals. *American Journal of Science* **267**, 43–63.
- Mueller, K. J. (1992). Tertiary basin development and exhumation of the northern East Humboldt–Wood Hills metamorphic complex, Elko County, Nevada. Unpublished Ph.D. thesis, University of Wyoming.
- Mueller, K. J. and Snoke, A. W. (1993) Progressive overprinting of normal fault systems and their role in Tertiary exhumation of the East Humboldt–Wood Hills metamorphic complex, northeast Nevada. *Tectonics* **12**, 361–371.
- Northrup, C. J. (1996) Structural expressions and tectonic implications of general noncoaxial flow in the midcrust of a collisional orogen: The northern Scandinavian Caledonides. *Tectonics* **15**, 490–505.
- Oxburgh, E. R. and Turcotte, D. L. (1974) Thermal gradients and regional metamorphism in overthrust terranes with special reference to the eastern Alps. *Schweizerische Mineralogische und Petrographische Mitteilungen* **54**, 641–662.
- Ramsay, J. G. and Huber, M. I. (1983) *The Techniques of Modern Structural Geology, Volume 1: Strain Analysis*. Academic Press, London.
- Schmid, S. M. and Casey, M. (1986) Complete fabric analysis of some commonly observed quartz *c*-axis patterns. In *Mineral and rock deformation studies, the Paterson Volume*, eds B. E. Hobbs and H. C. Heard, pp. 263–286. American Geophysical Union, Geophysical Monograph, **36**.
- Simpson, C. (1986) Determination of movement sense in mylonites. *Journal of Geological Education* **34**, 246–261.
- Simpson, C. and Schmid, S. M. (1983) An evaluation of criteria to deduce sense of movement in sheared rocks. *Geology* **94**, 1281–1288.
- Snoke, A. W. and Lush, A. P. (1984) Polyphase Mesozoic–Cenozoic deformational history of the Ruby Mountains–East Humboldt Range, Nevada. In *Western geological excursions: Geological Society of America annual meeting field trip guidebook*, ed. J. Lintz Jr, pp. 232–260. Mackay School of Mines, Reno, **4**.
- Snoke, A. W., McGrew, A. J., Valasek, P. A. and Smithson, S. B. (1990) A crustal cross section for a terrain of superimposed shortening and extension: Ruby Mountains–East Humboldt Range Nevada. In *Exposed Cross Sections of the Continental Crust*, eds M. H. Salisbury and D. M. Fountain, pp. 103–135. Kluwer Academic Publishers, Boston.
- Thompson, A. B. and England, P. C. (1984) Pressure–temperature–time path of regional metamorphism II. Their inference and interpretation using mineral assemblages in metamorphic rocks. *Journal of Petrology* **25**, 929–955.
- Turcotte, D. I. and Schubert, G. (1982) *Geodynamics Applications of Continuum Physics to Geological Problems*. John Wiley and Sons, New York.
- Wells, M. L. (1997) Alternating contraction and extension in the hinterlands of orogenic belts: an example from the Raft River Mountains, Utah. *Geological Society of America Bulletin* **109**, 107–126.
- Wells, M. L. and Allmendinger, R. W. (1990) An early history of pure shear in the upper plate of the Raft River metamorphic core complex: Black Pine Mountains, southern Idaho. *Journal of Structural Geology* **12**, 851–867.